The Measurement of Circular Polarization in the Near-IR Luminescence from Chiral Complexes of Yb(III) and Nd(III)

Christine L. Maupin,[†] Rachel S. Dickins,[‡] Linda G. Govenlock,[‡] Celine E. Mathieu,[‡] David Parker,[‡] J. A. Gareth Williams,[‡] and James P. Riehl*[,†]

Department of Chemistry, Michigan Technological University, Houghton, Michigan 49931, and Department of Chemistry, University of Durham, South Road Durham, U.K. DH1 3LE

Received: February 18, 2000; In Final Form: May 22, 2000

This work describes the measurement and analysis of circular polarization in the luminescence (CPL), in the near-IR spectral region, from chiral complexes of Yb(III) and Nd(III) in solution. The experimental technique is based upon previous measurements of CPL in the visible region. Instrumentation design, performance, and calibration are discussed. The experimental technique has been applied to several related complexes of Yb(III) and Nd(III) with chiral macrocyclic ligands based on 1,4,7,10-tetraazacyclododecane that have approximate C_4 symmetry. In addition, CPL from D_3 complexes of Yb(III) with 2,6-pyridinedicarboxylate, which were prepared as a solution of enriched enantiomers by the addition of (+)-dimethyltartrate, is also presented. It is demonstrated that CPL from the $^2F_{5/2} \rightarrow {}^2F_{7/2}$ transition of Yb(III) at 980 nm is particularly suited for CPL studies because this transition satisfies magnetic-dipole selection rules. The luminescence from the $^4F_{3/2} \rightarrow {}^4I_{9/2}$ and $^4F_{3/2} \rightarrow {}^4I_{11/2}$ transitions of Nd(III) centered at 880 and 1060 nm, respectively, showed only weak CPL signals. The usefulness of these types of polarization measurements in the near-IR is discussed.

1. Introduction

The measurement of circular polarization in the luminescence (CPL) from chiral molecules is one of a small number of modern spectroscopic techniques that are being used as specific, direct probes of chiral structure.[1,2] Although the number and scope of applications of CPL is increasing, it is certainly the case that this technique has not been as widely used as circular dichroism (CD) spectroscopy, which measures the difference in absorption of circularly polarized light. One reason for the disparate application of these two chiroptical techniques is the fact that no commercial CPL instrument is currently available, whereas there are several manufacturers of CD instruments. It is also the case that, in CPL spectroscopy, one is limited to chiral luminescent species of which there are far fewer than there are chiral absorbers. Most of the recent applications of CPL have, in fact, exploited this selectivity and the inherent sensitivity that luminescence measurements have over absorption measurements.

Although the range of previous and potential applications of CPL spectroscopy is fairly broad, the class of chiral systems for which the CPL technique has been especially suited is the study of chiral complexes containing luminescent lanthanide(III) ions. In particular, CPL studies involving chiral complexes containing Eu(III) and Tb(III), and to a lesser extent Dy(III) and Sm(III), have been reported and have been shown to provide unique information concerning the chiral structure and dynamics of important and interesting chemical systems.[3−11] These ions all luminesce in the visible region of the spectrum. One of the characteristics of lanthanide(III) ions that makes them ideal targets for CPL studies is the availability of absorption and emission intraconfigurational f ↔ f transitions between states that satisfy magnetic-dipole selection rules. These transitions are often associated with large chiral discrimination in absorption and emission.[12] All of the available f ↔ f transitions are formally Laporte forbidden; however, the weak absorption of these ions may be overcome with high-power laser excitation or, in many cases, with indirect excitation of aromatic chromophores followed by energy transfer to an excited state of the lanthanide ion.

There has been one published report on an attempt to measure CPL in the near-IR region. Morita and Herren examined the near-IR luminescence from Er(III) doped into a single chiral crystal of $Gd_2(MoO_4)_3$, which was prepared under conditions in which the high-temperature orthorhombic β' phase is produced.[13] In this crystal, two different Gd(III) sites are present, both with C_1 symmetry. Luminescence from Er(III) from the two sites in the crystal at low temperature was analyzed for linear polarization and circular polarization. Some qualitative evidence for circularly polarized luminescence was observed, although in this experimental procedure, a conventional photoelastic polarization modulator could not be used because of the spectral region of interest (1.53 μm). To produce a modulated polarization analyzer for this region, they combined a quarter-wave plate with alternating horizontal and vertical polarizers attached to an optical chopping device. It is well-known that the mechanical switching of alternating polarizers and even slight differences in optical alignment may produce an artifact because of linear polarization that will be indistinguishable from circularly polarized light, so verification of these results through the measurement of the enantiomeric crystal is necessary.[14]

In this work, we report on the first series of CPL measurements from solutions of chiral complexes containing Yb(III) and Nd(III), which both luminesce in the near-IR. A preliminary report of this work has already been published.[8] The motivation for this work is the recent increased interest in the area of intrinsic biomolecule luminescence and fluorescent labeling of

* Author to whom correspondence should be addressed.
[†] Michigan Technological University.
[‡] University of Durham.

10.1021/jp000648y CCC: $19.00
Published on Web 07/01/2000

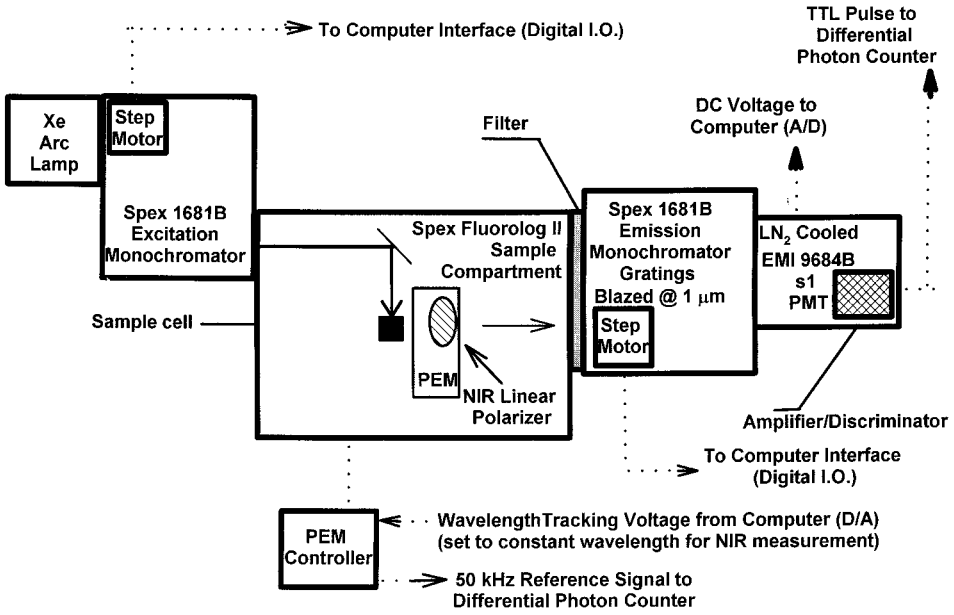

Figure 1. Schematic diagram for instrumentation used to measure circularly polarized luminescence in the near-IR spectral region.

biomolecules in the near-IR spectral region. Of special importance in these current and potential applications is the fact that skin, tissue, blood, and serum are essentially transparent in the near-IR region.[15−17] Furthermore, many samples that appear to be cloudy or hazy in visible light are comparatively nonscattering in the near-IR region because of the ν^4 dependence of the intensity of scattered light, allowing for much deeper penetration of a probe beam.

2. Experimental Section

Sample Preparation. The NMR chiral shift reagent Yb(III) tris[3-(trifluoromethylhhydroxymethylene)-(+)-camphorate], Yb(facam)$_3$, was purchased as a solid from Aldrich Chemical and used without purification. Samples for spectroscopic measurements were prepared in a 0.4-cm path length quartz fluorescence cuvette. A solution of Yb(facam)$_3$ was prepared by dissolving weighed amounts (0.0080 g) of the solid compound in 1.00 mL of dimethyl sulfoxide (DMSO).

2,6-Pyridinedicarboxylic acid (dipicolinic acid = DPA) was purchased from Aldrich Chemical and used without further purification. Weighed amounts of the solid acid were dissolved in distilled water, and the pH was adjusted to approximately 9 through the addition of NaOH. The final concentration of the stock solution of DPA^{2-} was 0.18 M. Yb(III) chloride hexahydrate ($YbCl_3$) was purchased from Acros and also used without further purification. The $YbCl_3$ solid was dissolved in distilled water, and the pH was adjusted to 3 with HCl. The final stock solution of $YbCl_3$ was 0.14 M. Solutions of $Yb(DPA)_3^{3-}$ with a final concentration 0.03 M and a pH of approximately 8 were made by mixing appropriate volumes of the stock solutions. In experiments involving the use of a Pfeiffer agent, 25 g of dimethly-L-tartrate (+DMT) (Aldrich) was added to10 mL of 0.03 M $Yb(DPA)_3^{3-}$ in 5 g portions while the solution was being constantly stirred and very gently heated. The final concentration of $Yb(DPA)_3^{3-}$ for these measurements was 0.01 M, and the concentration of (+DMT) was 4.7 M with a pH of approximately 8. All measurements involving $Yb(DPA)_3^{3-}$ were performed in a quartz fluorescence cuvette with a path length of 0.4 cm.

Chiral macrocyclic tetraamide ligands based on 1,4,7,10-tetraazacyclododecane were prepared as described previously.[10] Solutions of $Yb(Rphen)_4^{3+}$ and $Yb(Sphen)_4^{3+}$ were prepared by dissolving the trifluoromethanesulfonate (triflate) salt in a small amount of acetonitrile or methanol and adding D_2O to obtain a final volume of 0.8 mL.

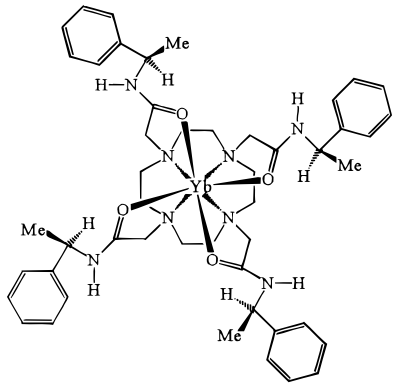

$Yb(Rphen)_4^{3+}$

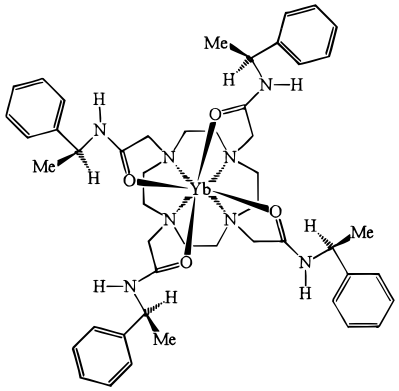

$Yb(Sphen)_4^{3+}$

The R and S nomenclature employed above is used only to specify the chirality of the asymmetric amine carbon. For these complexes, it has been shown that, in fact, the configuration of the chiral center in the amide group also determines the

macrocyclic ring conformation and the helicity of the pendant arms. The R configuration at carbon leads to formation of a single C_4-symmetric enantiomer with Λ helicity that is rigid on the time scale of luminescence.[18] Solutions of Yb(RBrphen)$_4^{3+}$ and Yb(SBrphen)$_4^{3+}$ were prepared in a similar manner.

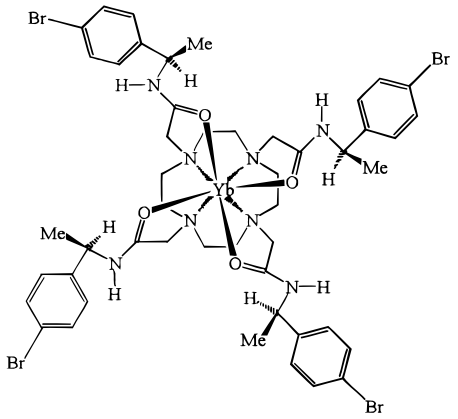

Yb(RBrphen)$_4^{3+}$

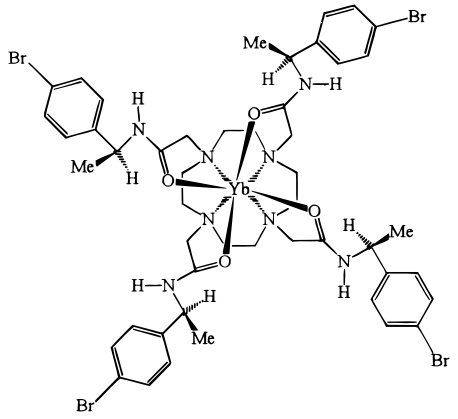

Yb(SBrphen)$_4^{3+}$

Complexes in which one of the chiral pendant amide groups was replaced with an achiral phenanthridine (phenan) moiety were prepared as described previously.[19] Solutions were prepared by dissolving the triflate salts in a small amount of acetonitrile or methanol and adding D_2O to obtain a final volume of 0.6 mL. All solutions were degassed, and the pH was adjusted to $\leq$2.5 by addition of a drop of trifluoroacetic acid (Aldrich Chemical). Protonation of the phananthridine nitrogen serves to enhance the absorbance of the complex at the excitation wavelength.[19]

Also studied were complexes of Nd(III) and Yb(III) in which one of the pendant chiral amines was replaced by a Pd-centered porphyrin complex (PdPorph).[20] In these experiments, the $CF_3SO_3^-$ salts were dissolved in EtOH.

All samples were prepared and measured in quartz fluorescence cuvettes.

Instrumentation. A schematic diagram of the instrumentation used to measure circular polarization in the near-IR is presented in Figure 1. As illustrated, these measurements were made using the 450-W Xe arc-lamp excitation source, monochromators, and sample compartment of a commercial Spex Fluorolog II spectrofluorimeter. The design of the instrumentation is very similar to that used to measure CPL in the visible region.[2]

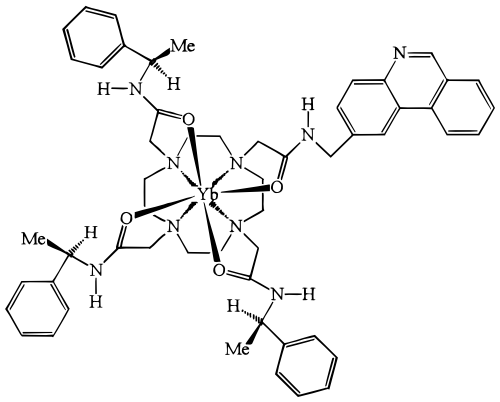

Yb(RBrphen)$_3$(phenan)$^{3+}$

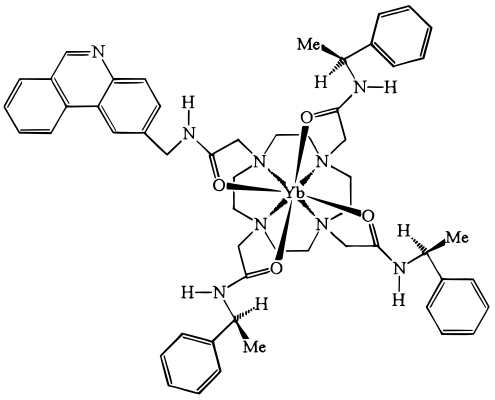

Yb(SBrphen)$_3$(phenan)$^{3+}$

Circular polarization in the luminescence is detected through a 50-kHz photoelastic modulator (PEM) that is set to operate as an oscillating quarter-wave plate. The PEM was placed in the sample compartment in close proximity to the cuvette containing the luminescent sample. For these measurements, a high-quality near-IR linear polarizer is attached to the PEM to convert the alternately left and then right circularly polarized near-infrared light to linearly polarized light. The PEM controller was manually set to the wavelength in the middle of the narrow spectral range of the emitted light [980 nm for Yb(III) and 1040 nm for Nd(III)]. The intensity of the modulated linearly polarized light will vary at 50 kHz if the luminescence is

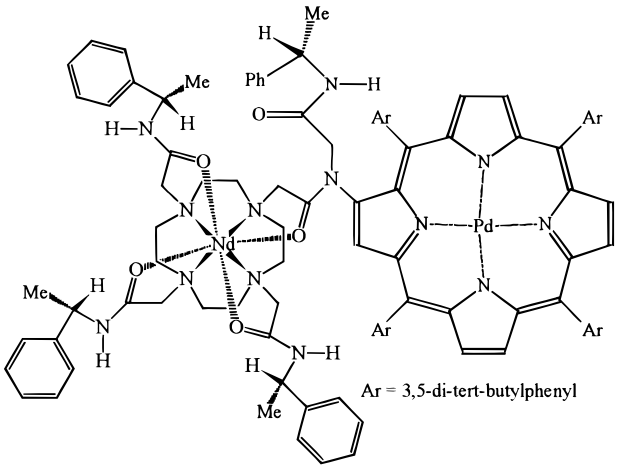

Nd(Rphen)$_3$(PdPorph)$^{3+}$

partially circularly polarized. The emission beam was focused onto the adjustable entrance slits of a Spex 1681B monochromator blazed at 1 μm and classically grooved with 600 gr/mm and a 3.77 nm/mm dispersion. Calibration of the emission monochromator was accomplished by scattering a small amount of a He−Ne laser beam through the detection optics. Background signal from stray excitation and room light was reduced by placement of a long-pass filter in the light path of the emission, prior to its entering the monochromator. The exit slit compartment of the emission monochromator was directly attached to a sealed shutter, and a liquid-nitrogen-cooled photomultiplier housing, which was operated at −100 °C. The shutter assembly was sealed by the insertion of rubber o-rings between the mechanical connections of the monochromator and the photomultiplier housing. The photomultiplier tube used in this work was an EMI 9684B with an S-1 spectral response. The front window of the photomultiplier housing is a hermetically sealed double-plated ultralow radio-isotope borosilicate window that is electrically heated to control dew or frost accumulation. The photomultiplier tube was operated at a voltage of approximately 1500 V in photon-counting mode.

The output of the photomultiplier tube was amplified by an Advanced Research Instruments Corporation combination amplifier−discriminator (Combo-100 Preamplifier V6), which was attached by a very short (4 in.) BNC cable. This device provides simultaneous DC and photopulse output. Electronic TTL pulses are generated from the photon spikes, as well as a DC signal proportional to the total emission intensity. The TTL pulses are input to a custom-built gated differential photon counting (DPC) system, which is driven by a reference signal from the PEM. On alternate half cycles of the 50-kHz modulation period, an up/down counter is switched so that, when the PEM is transmitting left circularly polarized light, the TTL pulses are added, and when right circularly polarized light is being transmitted, the TTL pulses are subtracted. The DPC also contains a counter that monitors the total photon count. For all of the measurements reported here, the counts were collected during a time window centered at the peak of the modulation cycle and for a period corresponding to 50% of the available time. Inclusion of TTL pulses that are detected off center to this degree from pure quarter-wave retardation results in a small (<5%) error in the final result. The DPC and emission monochromator are interfaced to a dedicated personal computer for data analysis and instrument control.

3. Excitation of Yb(III) and Nd(III)

Approximate energy level diagrams for the f electronic states of Yb(III) and Nd(III) free ions are displayed in Figure 2. As can be seen, the energy level diagram for Nd(III) is composed of numerous $^{2S+1}L_J$ terms arising from the $4f^3$ electron configuration, whereas the very simple energy level diagram for Yb(III) results from the electron configuration $4f^{13}$. Because the intraconfigurational f ↔ f transitions are forbidden, excitation (absorption) of lanthanide(III) is very weak; in most cases, one must use either high-power laser excitation sources or indirect excitation of strongly absorbing ligands followed by energy transfer to promote the lanthanide(III) ions to the emitting state. Indirect excitation of Tb(III) and Eu(III) via absorption of aromatic ligands is quite common and efficient in those cases where the energy of the triplet state of the ligand is situated slightly above (~1700 cm^{-1}) an excited lanthanide ion electronic state. If the triplet energy level is above, but closer than 1700 cm^{-1}, the luminescence is decreased because of back energy transfer from the metal ion to the ligand. If the aromatic triplet state is located slightly below the emitting state, then energy back transfer from metal to ligand may result in little or no emission from the lanthanide(III) ion.

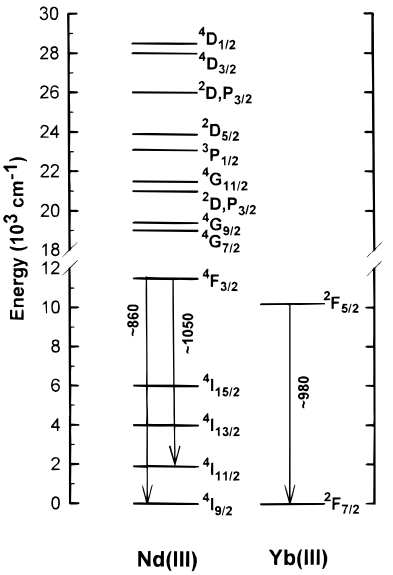

Figure 2. Approximate free-ion energy levels for Nd(III) and Yb(III).

The indirect excitation of Nd(III) via strongly absorbing ligands is quite feasible because there are so many f electronic states (not all of them are shown in Figure 2) available in the spectral region (250−450 nm) in which one expects to find singlet and triplet transitions of organic aromatic ligands. However, on the basis of simple overlap arguments, it is not obvious that significant excitation of Yb(III) could be accomplished in the same manner. Nevertheless, there have been several reports of Yb(III) emission following indirect UV excitation.[21−24] Recently, Horrocks et al. have proposed that luminescence from a Yb(III) ion, which has been used as a substitutional replacement for the Ca(II) ion in cod-parvalbumin, results from an internal two-step redox process.[25] In this mechanism, an electron is transferred from the excited singlet state of tryptophan to the Yb(III) ion, forming Yb(II) and an excited tryptophan cation radical. Excited Yb(III) is then formed by back transfer of the electron to the tryptophan ligand. The second mechanism proposed by Beeby et al. is simply a very inefficient energy transfer process in the manner observed with the other luminescent lanthanide(III) ions.[26] With respect to this second excitation mechanism, it has been shown that, for a macrocyclic eight-coordinate tetraamide complex containing a phenanthridine ligand, the intramolecular energy transfer is the rate-determining step. These authors also report that, when the phenanthridine ligand is completely deprotonated at pH > 8, the lifetime of the Yb(III) emission becomes equal to the lifetime of the metal ion. They speculate that, under these conditions, the two-step redox mechanism may be operative, as deprotonation is accompanied by the appearance of an oxidation potential at 1.0 V. No oxidation wave was seen in cyclic voltammetry of phenanthridinium hydrochloride below 2.2 V, and the reduction of the related $Yb(R\text{-}phen)_4^{3+}$ complex occurs at potentials of more than −1.5 V, precluding the possibility of an electron-transfer mechanism.

All of the luminescence spectra reported in this work were accomplished with UV excitation from the Xe arc lamp. Representative excitation spectra are presented in Figure 3. In Figure 3A, we plot the excitation spectrum for $Yb(Sphen)_4^{3+}$ for the emission monitored at 980 nm. In Figure 3B, we show the excitation spectrum for a D_2O solution of $Yb(DPA)_3^{3-}$. This

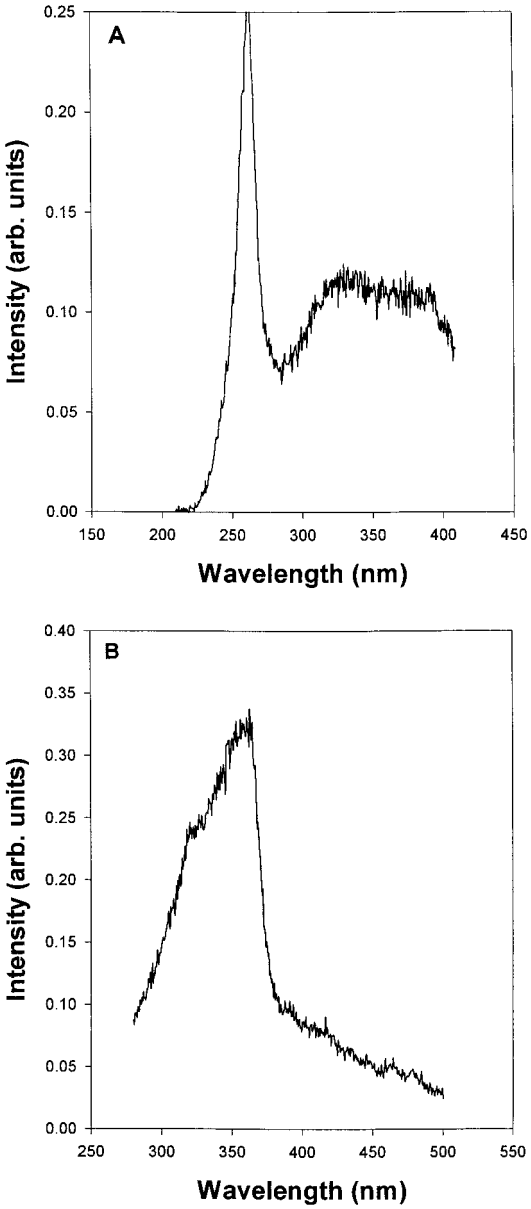

Figure 3. (A) Excitation spectrum for $Yb(Sphen)_4^{3+}$ in a methanol/D_2O mixture. (B) excitation spectrum for $Yb(DPA)_3^{3-}$ in D_2O. The emission was monitored at 980 nm.

excitation spectrum is essentially identical to that of $Eu(DPA)_3^{3-}$ and $Tb(DPA)_3^{3-}$.

4. Instrument Calibration

In CPL spectroscopy, it is common to report results in terms of the so-called luminescence dissymmetry factor, g_{lum}, which is defined as follows

$$g_{lum} \equiv \frac{\Delta I}{I/2} = \frac{I_L - I_R}{\frac{1}{2}(I_L + I_R)} \qquad (1)$$

where I_L and I_R refer, respectively to the intensity of left and right circularly polarized emitted light.[1] The factor of $^1/_2$ in this equation is added so that this definition is consistent with the corresponding quantity used in CD spectroscopy, g_{abs}, the absorption dissymmetry factor

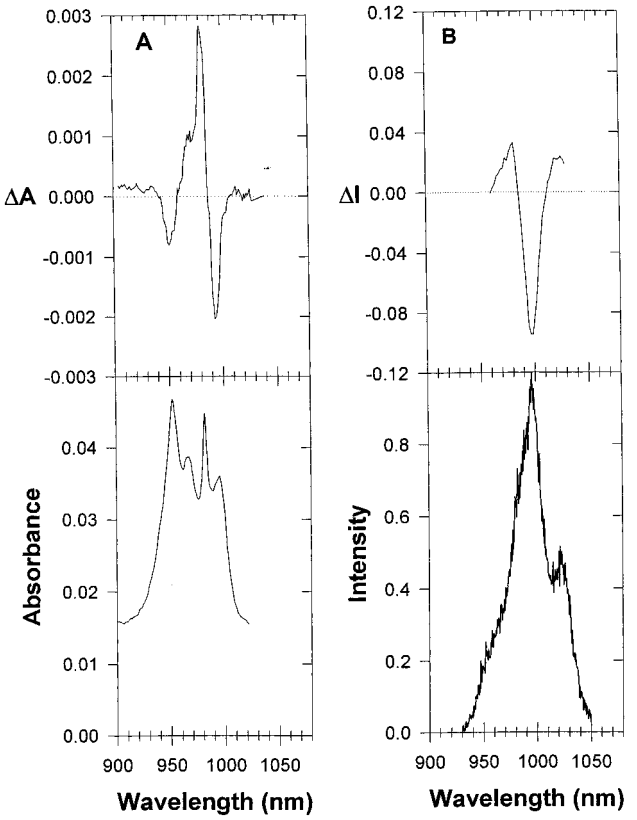

Figure 4. (A) Absorbance (lower curve) and differential absorbance (upper curve) for $Yb(Rphen)_4^{3+}$. (B) Luminescence (lower curve) and circularly polarized luminescence (upper curve) for $Yb(Rphen)_4^{3+}$. λ_{exc} = 260 nm.

$$g_{abs} \equiv \frac{\epsilon_L - \epsilon_R}{\frac{1}{2}(\epsilon_L + \epsilon_R)} = \frac{\Delta\epsilon}{\epsilon} = \frac{\Delta A}{A} \qquad (2)$$

where ϵ_L and ϵ_R correspond, respectively, to the extinction coefficient for left and right circularly polarized light, ϵ is the average extinction coefficient, and ΔA and A refer to the differential and average absorbance, respectively.

Calibration of the CPL instrumentation in the near-IR region can be performed if one is able to compare the CD of a stable chiral compound with the measured CPL of the same transition. The absorption (A) and differential absorption (CD) for the $^2F_{7/2} \rightarrow {}^2F_{5/2}$ transition of Yb(III) from a solution of $Yb(Rphen)_4^{3+}$ have been reported previously and are displayed in Figure 4A.[10] For comparison, the total luminescence (I) and differential luminescence (ΔI) for a solution of $Yb(Rphen)_4^{3+}$, measured using the instrumentation described above, are plotted in Figure 4B. The absorption and CD measurement was performed with slightly higher instrument resolution, but in both measurements, one can see a number of transitions corresponding to various crystal field transitions. In C_4 double-group symmetry, there are four possible crystal field ground-state doublets and three excited-state doublets. Note that the highest-energy absorption (950 nm), which probably corresponds to a transition to the highest-energy-level crystal state of the $^2F_{5/2}$ level, is not seen in emission as this state would not be populated at room temperature, and for the same reason, the lowest-energy luminescence transition (1025 nm), which probably corresponds to a transition to the highest-energy crystal field state of the $^2F_{7/2}$ ground-state term, is not seen in absorption. Obviously, the spectra displayed correspond to a complicated overlap of the various transitions with differing thermal populations. It is,

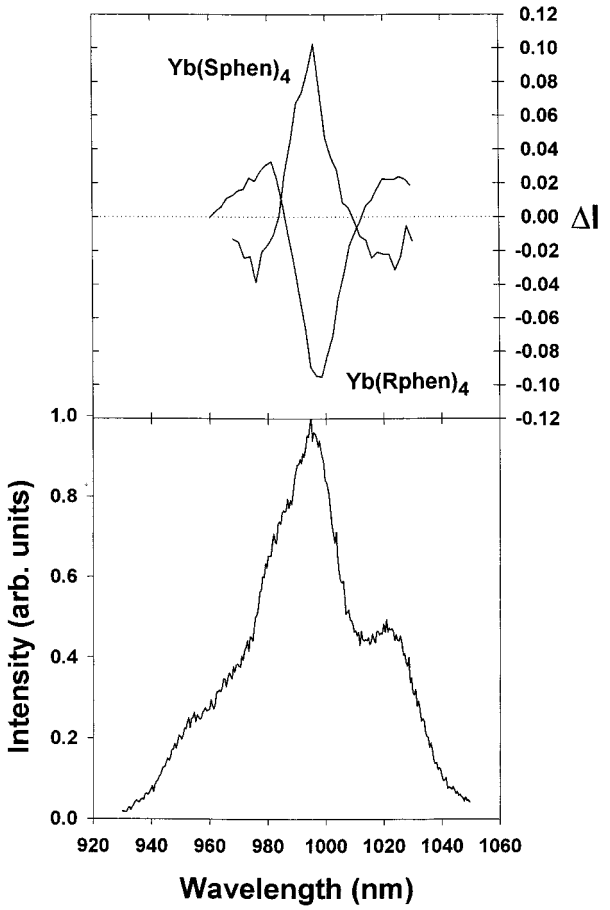

Figure 5. Circularly polarized luminescence (upper curves) and total luminescence (lower curve) for solutions of $Yb(Rphen)_4^{3+}$ and $Yb(Sphen)_4^{3+}$ in a MeOH/D_2O mixture. The total luminescence signals from the enantiomeric solutions was virtually identical, and therefore, only one is shown. $\lambda_{exc} = 260$ nm.

therefore, not possible to make a quantitative comparison of the CD and CPL for an isolated transition.

These results may, however, be used to verify the sign of the CPL measurement, and they are also useful as a qualitative measure of magnitude. For example, the peak corresponding to the maximum luminescence (995 nm) is associated with a g_{lum} value of -0.18. This peak corresponds to the highest-wavelength peak in the absorption spectrum with g_{abs} equal to -0.11 after baseline subtraction. The same sign is what one expects for the same transition, and the order of magnitude of the dissymmetry factors are similar. Quantitative determination of g_{abs} is often difficult because of baseline problems, particularly in this spectral region. Further demonstration that the instrumentation is functioning properly can be obtained by measurement of CPL from enantiomeric complexes. These results are presented in Figure 5 for $Yb(Rphen)_4^{3+}$ and $Yb(Sphen)_4^{3+}$. As can be seen, mirror-image CPL spectra are obtained, consistent with the result expected for an instrument that is working properly.

Although the macrocyclic complex $Yb(Rphen)_4^{3+}$ is an excellent complex for testing the CPL instrumentation, it is not suitable as a standard calibrating agent because it is not commercially available. We have chosen to use a solution of tris[3-(trifluoromethylhydroxymethylene)-d-camphorato]ytterbium(III), $Yb(facam)_3$ (Aldrich), prepared in dry dimethyl sulfoxide (DMSO) for this purpose. The Eu(III) analogue of this complex is used as a standard in CPL measurements in the visible region.[2] The total and circularly polarized luminescence

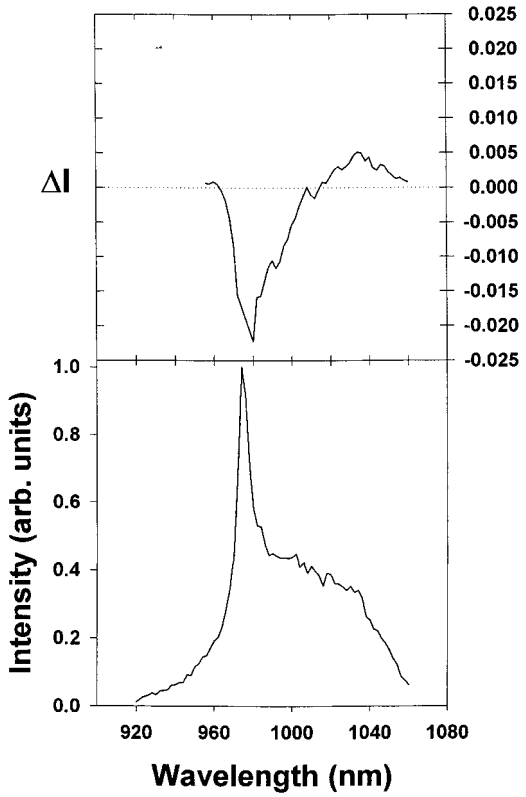

Figure 6. Circularly polarized luminescence (upper curve) and total luminescence (lower curve) for a solution of $Yb(facam)_3^{3+}$ in DMSO. $\lambda_{exc} = 360$ nm.

of this compound are plotted in Figure 6. This species has a measured g_{lum} value of -0.076 at the peak wavelength (975 nm). This Yb(III) complex is very soluble in DMSO, and calibration solutions can be prepared simply by dissolving the solid sample in DMSO. It should be noted that the solvent must be dry, because the addition of even small amounts of water will significantly alter the value of g_{lum}. The $Yb(facam)_3$ solution was excited at 365 nm, and the luminescence was collected with a spectral band-pass of 0.9 nm for the spectra shown in Figure 6.

5. Results and Discussion

In Figures 7, we plot total luminescence (lower curve) and circularly polarized luminescence (upper curve) for the complex $Yb(SBrphen)_4^{3+}$. A comparison of the CPL spectrum with that of the parent complex $Yb(Sphen)_4^{3+}$, given in Figure 5, shows that the addition of the *para*-Br substituent has only a small effect on the chirality of the Yb(III) emission, and the overall pattern of the CPL is unchanged. This result suggests that the C_4 environments around the metal ion are very similar. The peak of the excitation spectrum for $Yb(SBrphen)_4^{3+}$ was 296 nm, compared to 260 nm for $Yb(Sphen)_4^{3+}$. Part of the motivation for preparing derivatives of the parent complex is an effort to move the excitation of these potential luminescent bio-probes out of the UV region.

It must be mentioned that the luminescence dissymmetry factor, g_{lum}, obtained from these complexes is very large. At the peak of the luminescence, we obtain values of approximately ± 0.2. For purposes of comparison, even for very highly constrained chiral organic chromophores, it is very unusual to measure $|g_{lum}|$ values greater than 0.005; however, these magnitudes are observed for transitions in lanthanide(III) ions that obey magnetic-dipole selection rules $\Delta J = 0, \pm 1$. The $^2F_{7/2}$

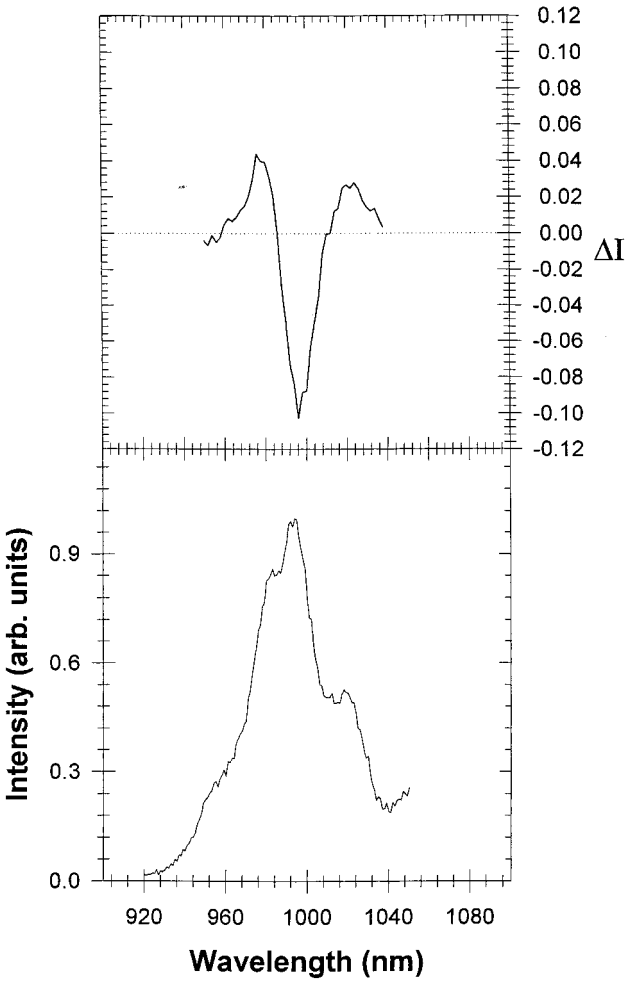

Figure 7. Circularly polarized luminescence (upper curve) and total luminescence (lower curve) for a solution of $Yb(RBrphen)_3^{3+}$ in a $MeOH/D_2O$. $\lambda_{exc} = 296$ nm.

$\leftrightarrow$ $^2F_{5/2}$ transition of Yb(III) is magnetic-dipole-allowed, and the large g_{lum} value obtained in many of these complexes is consistent with previous NMR solution observations showing that the complexes are fairly rigid and stable on the luminescence time scale.[18]

In Figure 8, the total luminescence (lower curve) and circularly polarized luminescence (upper curve) have been plotted for the enantiomeric pair Λ-$Yb(Rphen)_3(phenan)^{3+}$ and Δ-$Yb(Sphen)_3(phenan)^{3+}$, in which one of the chiral amine groups has been replaced with an achiral aromatic phenanthridine group. For this complex, excitation at 355 nm results in population of the $^2F_{7/2}$ emitting state of Yb(III). As can be seen by comparison with the results plotted in Figure 5, this substitution has only a small effect on the magnitude of g_{lum}. The conclusion that the overall C_4 symmetry surrounding the central lanthanide(III) ion is essentially determined by only three chiral arms is consistent with results obtained previously from Eu(III) and Tb(III) analogues of these complexes.[19,27]

In Figure 9A and B, we plot total luminescence and CPL results for complexes in which one of the chiral amine appendages has been substituted with a Pd-centered porphyrin. In Figure 9A, we plot results for the complex $Yb(Rphen)_3(Pdporph)^{3+}$ in which three of the amines are of the R configuration, and in Figure 9B, we show CPL results for the enantiomer of this molecule, $Yb(Sphen)_3(Pdporph)^3$. By comparing these results again to the spectra plotted in Figure 4, we see considerable broadening of the total luminescence spectrum,

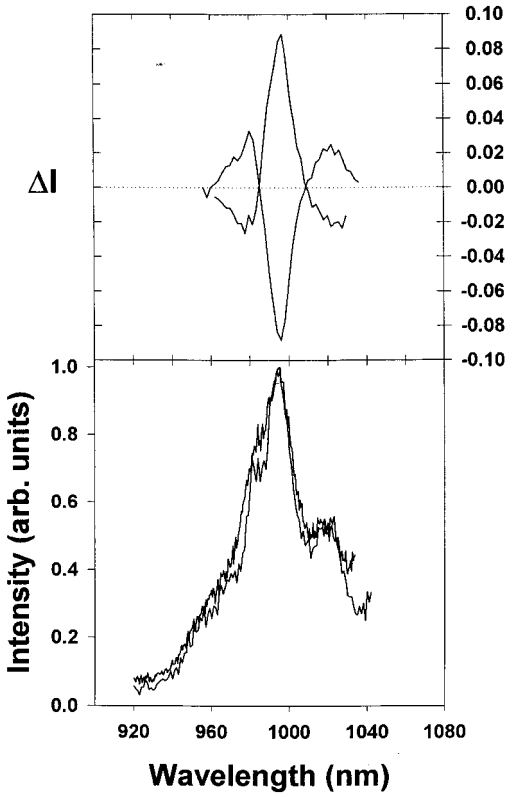

Figure 8. Circularly polarized luminescence (upper curves) and total luminescence (lower curves) for solutions of $Yb(Rphen)_3(phenan)^{3+}$ and $Yb(Sphen)_3(phenan)^{3+}$ in an acidified $MeOH/D_2O$ mixture. $\lambda_{exc} = 355$ nm.

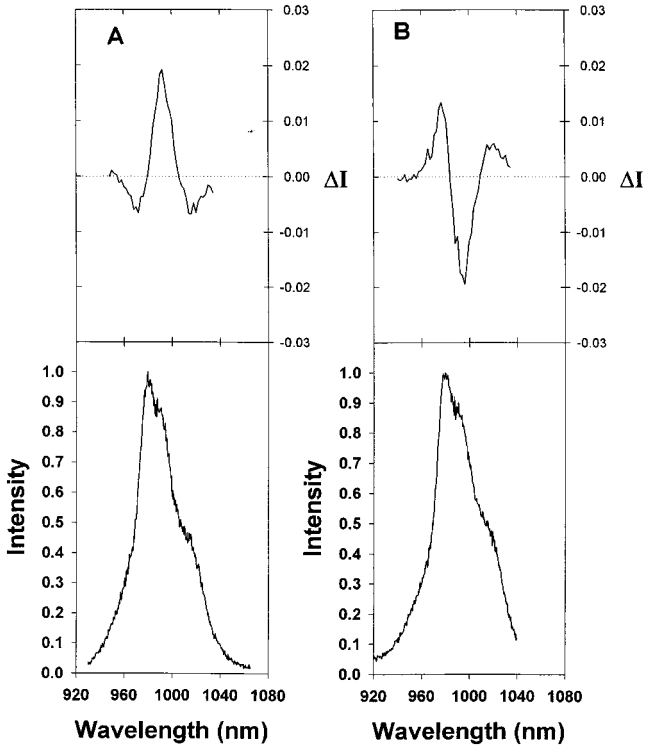

Figure 9. (A) Total luminescence (lower curve) and circularly polarized luminescence (upper curve) for $Yb(Sphen)_3(Pdporph)^{3+}$ in ethanol. (B) Total luminescence (lower curve) and circularly polarized luminescence (upper curve) for $Yb(Rphen)_3(Pdporph)^{3+}$. $\lambda_{exc} = 415$ nm.

and a shift of the maximum intensity to lower wavelength. These kinds of spectral changes are not unexpected for such a large

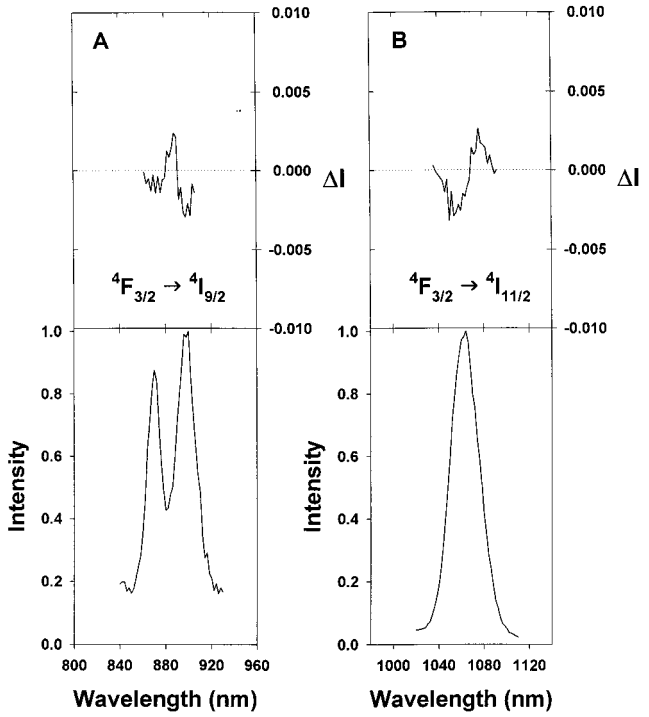

Figure 10. Total luminescence (lower curve) and circularly polarized luminescence (upper curve) for two transitions of $Nd(Rphen)_3(Pdporph)^{3+}$ in ethanol. (A) $^4F_{3/2} \rightarrow {}^4I_{9/2}$, and (B) $^4F_{3/2} \rightarrow {}^4I_{11/2}$. $\lambda_{exc} = 415$ nm.

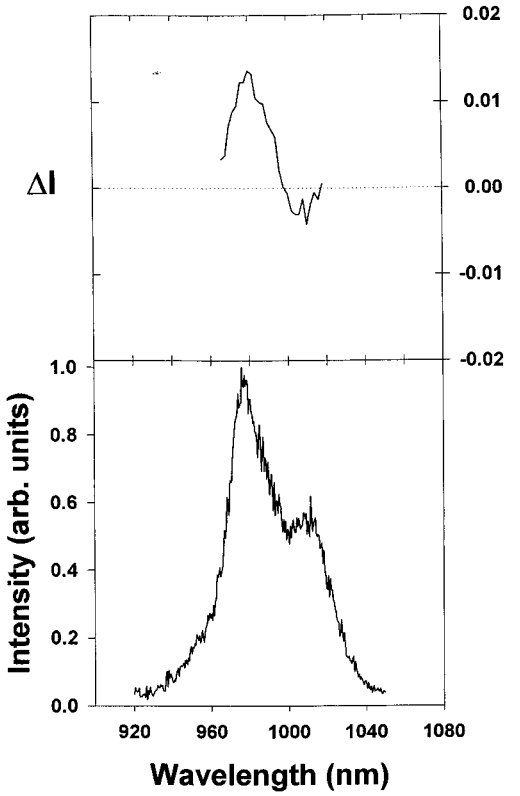

Figure 11. Circularly polarized luminescence (upper curve) and total luminescence (lower curve) for a solution of $Yb(DPA)_3^{3-}$ in D_2O following the addition of 4.7 M (+)-dimethyltartrate. $\lambda_{exc} = 330$ nm.

modification of the parent structure. It is somewhat remarkable that the same CPL sign pattern is still obtained, indicating that the helicity of the C_4 twist is still maintained to some extent in this complex.

In Figure 10A and B, we show the total luminescence and CPL spectra obtained from $Nd(Rphen)_3(Pdporph)^{3+}$ for the transitions $^4F_{3/2} \rightarrow {}^4I_{9/2}$ and $^4F_{3/2} \rightarrow {}^4I_{11/2}$, respectively. The luminescence in the near-IR region from this complex is easily measured; however, the circularly polarized luminescence is small. Because neither of these transitions satisfy magnetic-dipole selection rules, the small g_{lum} values obtained are not unexpected. Even though the chirality of these transitions is not large, the measurement of CPL from chiral Nd(III) complexes may be quite useful, as it is one of the few lanthanide(III) ions for which absorption and CD measurements are fairly routine. In particular, quantitative measurements involving the hypersensitive $^4I_{9/2} \rightarrow {}^4G_{5/2}$ transition have been quite useful in probing the structure of Nd(III) complexes.[28]

In Figure 11, the total luminescence (lower curve) and circularly polarized luminescence (upper curve) have been plotted for a solution of $Yb(DPA)_3^{3-}$ into which (+)-dimethyltartrate has been added, such that the final concentration was 4.7 M (+)-DMT. (+)-DMT has been known to perturb the equilibrium between interconverting enantiomers.[29] This perturbation of a racemic equilibrium is often referred to as the Pfeiffer effect.[30] Excitation of Yb(III) was accomplished through indirect excitation of the ligand at 330 nm. The spectral bandpass for the spectra shown was 4.7 nm. Note that the CPL of a solution of this complex without the addition of the (+)-DMT was not measurable. Complexes of this ligand with Eu(III), Tb(III), Dy(III), and other lanthanides are well-known.[31,32] These complexes occur in solution as interconverting D_3 enantiomers (Δ and Λ); however, the racemization is slow even compared to that of the ion with the longest luminescence lifetime [Tb(III), ~4 ms]. [The measurement of a g_{lum} value equal to 0 from the racemic mixture of $Yb(DPA)_3^{3-}$ is further evidence that the instrument is working correctly.] It is possible to determine an approximate value for the luminescence dissymmetry factor of a pure enantiomer of $Yb(DPA)_3^{3-}$ by using CPL and CD results from lanthanide(III) analogues.[32] The value of g_{lum} for the pure enantiomer can be related to the value measured from the enriched sample through the following equation

$$g_{lum}(\lambda) = \eta g^{\Delta}_{lum}(\lambda) \qquad (3)$$

where η is the enantiomeric excess produced by the addition of the (+)-DMT.

It has been previously determined that addition of 4.7 M (+)-DMT to a solution of $Dy(DPA)_3^{3-}$ yields an enantiomeric excess of 0.4.[33] Under the reasonable assumption that the solution properties of this complex are very similar to the Yb(III) complex, one can calculate, using eq 3, that the luminescence dissymmetry ratio at the peak of the emission for the pure Λ-enantiomer would be +0.075. This value is smaller than the value that was determined for the magnetic-dipole-allowed $^5D_0 \rightarrow {}^7F_1$ transition of Eu(III) (~0.45). This Eu(III) transition contains many fewer crystal field components than the corresponding transition of Yb(III), in which there exists a number of overlapping transitions, and as a result, a somewhat smaller value for g_{lum} is not surprising.

6. Summary and Conclusions

The results presented and discussed above show that the modifications that we have made to our CPL instrumentation has led to an accurate and reproducible method of measuring the luminescence dissymmetry ratios of complexes in the near-IR spectral region. For the most emissive systems that we have studied, at reasonable concentrations, the measured photon-count rate was approximately 10^3 counts/sec. It has been shown that,

for the differential photon-counting method operating under Poisson photon statistics, the standard deviation in the measured values of g_{lum} is equal to $1/N^{1/2}$, where N is the total number of photons counted.[34] Therefore, to determine the g_{lum} value at one wavelength with a standard deviation of 0.01 using a collection window of 50% requires only 20 s. Obviously, samples that are less emissive, or transitions with smaller intrinsic dissymmetry factors, will require correspondingly longer collection times.

The results presented here show that measurement of CPL from chiral Yb(III) complexes is certainly feasible and may represent a novel approach to the development of useful chiral assays of biological structure. In particular, it is demonstrated that the Yb(III) excited state may be populated through radiationless energy transfer from strongly absorbing ligands, yielding sufficient luminescence intensity for this type of polarization measurement.

Very recently, some of these and related Yb(III) complexes and their Eu(III) and Tb(III) analogues have been used in studies that demonstrate their potential to selectively bind to DNA.[27] In these preliminary studies, it was determined that the Δ-Eu complex binds strongly to calf-thymus DNA, and the binding to the oliginucleotide $[(CG)_6]_2$ was 50 times larger than binding to $[(AT)_6]_2$. A different pattern of binding affinity was exhibited by the Λ enantiomer, and this selectivity in binding must be due, in some way, to complementary properties that allow their interactions with chiral polyanions. By creating complexes that can bind to specific sites in the DNA helix, improved selective luminescent assays and the development of selectively reactive complexes may be possible.[27]

Acknowledgment is made to the EPSRC (D.P.) and to the Graduate School of Michigan Technological University (J.P.R.) for partial support of this work.

References and Notes

(1) Riehl, J. P.; Richardson, F. S. *Methods Enzymol.* **1993,** *226*, 539.
(2) Riehl, J. P.; Richardson, F. S. *Chem. Rev.* **1986**, *86*, 1.
(3) Hilmes, G. L.; Çoruh, N.; Riehl, J. P. *Inorg. Chem.* **1988**, *27*, 1136−1139.
(4) Metcalf, D. H.; Snyder, S. W.; Wu, S.; Hilmes, G. L.; Riehl, J. P.; Demas, J. N.; Richardson, F. S. *J. Am. Chem. Soc.* **1989**, *111*, 3082−3083.
(5) Rexwinkel, R. B.; Meskers, S. C. J.; Riehl, J. P.; Dekkers, H. P. J. M. *J. Phys. Chem.* **1992**, *96*, 1112−1120.
(6) Huskowska, E.; Maupin, C. L.; Parker, D.; Williams, J. A. G.; Riehl, J. P. *Enantiomer* **1997**, *2*, 381−395.
(7) Aime, S.; Botto, M.; Dickins, R. S.; Maupin, C. L.; Parker, D.; Riehl, J. P.; Williams, J. A. G. *J. Chem. Soc., Dalton Trans.* **1998**, 881−892.
(8) Maupin, C. L.; Parker, D.; Williams, J. A. G.; Riehl, J. P. *J. Am. Chem. Soc.* **1998**, *120*, 10563−10564.
(9) Dickins, R. S.; Howard, J. A. K.; Maupin, C. L.; Moloney, J. M.; Parker, D.; Peacock, R. D.; Riehl, J. P.; Siligardi, G. *New J. Chem.* **1998**, 891−898.
(10) Dickins, R. S.; Howard, J. A. K.; Maupin, C. L.; Moloney, J. M.; Parker, D.; Riehl, J. P.; Siligardi, G.; Williams, J. A. G. *Chem. Eur. J.* **1999**, 5.
(11) Belair, S. D.; Maupin, C. L.; Logue, M. W.; Riehl, J. P. *J. Lumin.* **2000**, *84*, 61−66.
(12) Richardson, F. S. *Inorg. Chem.* **1980**, *19*, 2806−2812.
(13) Herren, M.; Morita, M. *J. Lumin.* **1996**, *66*, 268.
(14) Dekkers, H. P. J. M.; Moraal, P.; Timper, J. M.; Riehl, J. P. *Appl. Spectrosc.* **1985**, *39*, 3203.
(15) Thompson, R. B. Red and Near-Infrared Fluorometry. *Topics in Fluorescence Spectroscopy*; Lakowicz, J. R., Ed.; Plenum Press: New York, 1994; Vol. 4, p 153.
(16) Casay, G. A.; Shealy, D. B.; Patonay, G. Near Infrared Fluorescence Probes. *Topics in Fluorescence Spectroscopy;* Lakowicz, J. R., Ed.; Plenum Press: New York, 1994; Vol. 4.
(17) Hemmila, A. *Applications of Fluorescence, Immunoassays*; Wiley: New York, 1991; Vol. 117.
(18) Batsanov, A. S.; Beeby, A.; Bruce, J. I.; Howard, J. A. K. Kenwright, A. M.; Parker, D. *J. Chem. Soc., Chem. Commun.* **1999**, 1011−1012.
(19) Parker, D.; Senanayake, P. K.; Williams, J. A. G. *J. Chem. Soc., Perkin Trans. 2* **1998**, 2129.
(20) Beeby, A.; Dickins, R. S.; Fitzgerald, S.; Govenlock, L. J.; Maupin, C. L.; Parker, D.; Riehl, J. P.; Siligardi, G.; Williams, J. A. G. *J. Chem. Soc., Chem. Commun.* **2000**, 1183−1184.
(21) Crosby, G. A.; Kasha, M. *Spectrochim. Acta* **1958**, *10*, 377.
(22) Perkins, W. G.; Crosby, G. A. *J. Chem. Phys.* **1965**, *42*, 407.
(23) Kachura, F. T.; Sevchenko, A. N.; Solov'ev, K. N.; Trvirko, M. P. *Dokl. Phys. Chem. (Engl. Transl.)* **1974**, *217*, 783.
(24) Gouterman, M.; Schumker, C. D.; Srivastava, T. V.; Yonetani, T. *Chem. Phys. Lett.* **1976,** *40*, 476.
(25) Horrocks, W.deW.; Bolender, J. P.; Smith, W. D.; Supkowski, R. M. *J. Am. Chem. Soc.* **1997**, *119*, 5972.
(26) Beeby, A.; Faulkner, S.; Parker, D.; Williams, J. A. G., to be published.
(27) Govenlock, L. J.; Mathieu, C. E.; Maupin, C. L.; Parker, D.; Riehl, J. P.; Siligardi, G.; Williams, J. A. G. *J. Chem. Soc., Chem. Commun.* **1999**, 1699−1700.
(28) Huskowska, E.; Riehl, J. P. *Inorg. Chem.* **1995**, *34*, 5615−21.
(29) Hilmes, G. L.; Çoruh, N.; Riehl, J. P. *Inorg. Chem.* **1988**, *27*, 3647.
(30) Pfeiffer, P.; Quehl, K. *Chem. Ber*. **1933**, *66*, 410.
(31) Hilmes, G. L.; Timper, J. M.; Riehl, J. P. *Inorg. Chem.* **1985**, *24*, 1721.
(32) Hilmes, G. L.; Riehl, J. P. *Inorg. Chem.* **1986**, *25*, 2617.
(33) Hilmes, G. L.; Çoruh, N.; Riehl, J. P. *Inorg. Chem.* **1988**, *27*, 1136−39.
(34) Schippers, P. H. Ph.D. Thesis, University of Leiden, Leiden, The Netherlands, 1972; Chapter 1.